

## Analysis of nonstationarity in renal autoregulation mechanisms using time-varying transfer and coherence functions

Ki H. Chon,<sup>1</sup> Yuru Zhong,<sup>1</sup> Leon C. Moore,<sup>2</sup> Niels H. Holstein-Rathlou,<sup>4</sup> and William A. Cupples<sup>3</sup>

Departments of <sup>1</sup>Biomedical Engineering and <sup>2</sup>Physiology and Biophysics, State University of New York at Stony Brook, Stony Brook, New York; <sup>3</sup>Department of Biology, University of Victoria, Victoria, BC, Canada; and <sup>4</sup>Department of Biomedical Sciences, University of Copenhagen, Copenhagen, Denmark

Submitted 11 August 2007; accepted in final form 19 May 2008

**Chon KH, Zhong Y, Moore LC, Holstein-Rathlou NH, Cupples WA.** Analysis of nonstationarity in renal autoregulation mechanisms using time-varying transfer and coherence functions. *Am J Physiol Regul Integr Comp Physiol* 295: R821–R828, 2008. First published May 21, 2008; doi:10.1152/ajpregu.00582.2007.—The extent to which renal blood flow dynamics vary in time and whether such variation contributes substantively to dynamic complexity have emerged as important questions. Data from Sprague-Dawley rats (SDR) and spontaneously hypertensive rats (SHR) were analyzed by time-varying transfer functions (TVTF) and time-varying coherence functions (TVCF). Both TVTF and TVCF allow quantification of nonstationarity in the frequency ranges associated with the autoregulatory mechanisms. TVTF analysis shows that autoregulatory gain in SDR and SHR varies in time and that SHR exhibit significantly more nonstationarity than SDR. TVTF gain in the frequency range associated with the myogenic mechanism was significantly higher in SDR than in SHR, but no statistical difference was found with tubuloglomerular (TGF) gain. Furthermore, TVCF analysis revealed that the coherence in both strains is significantly nonstationary and that low-frequency coherence was negatively correlated with autoregulatory gain. TVCF in the frequency range from 0.1 to 0.3 Hz was significantly higher in SDR (7 out of 7, >0.5) than in SHR (5 out of 6, <0.5), and consistent for all time points. For TGF frequency range (0.03–0.05 Hz), coherence exhibited substantial nonstationarity in both strains. Five of six SHR had mean coherence (<0.5), while four of seven SDR exhibited coherence (<0.5). Together, these results demonstrate substantial nonstationarity in autoregulatory dynamics in both SHR and SDR. Furthermore, they indicate that the nonstationarity accounts for most of the dynamic complexity in SDR, but that it accounts for only a part of the dynamic complexity in SHR.

hemodynamics; myogenic; tubuloglomerular feedback; hypertension

AUTOREGULATION OF RENAL BLOOD flow is mediated by the myogenic responses of the preglomerular vasculature (MYO) and the TGF feedback system. These two mechanisms exhibit characteristic resonant frequencies (MYO, 0.1–0.3 Hz; TGF, 0.02–0.05 Hz in rats). The marked difference in characteristic frequencies (and, hence, in time constants) between the TGF and MYO mechanisms permit separation and quantification of contributions of the two mechanisms by transfer function (1, 4, 29) and coherence analyses (2, 12).

A transfer function is the input-output relationship between an independent variable (blood pressure) and a dependent variable [renal blood flow (RBF)]. Its output is given in terms of gain, which reports fluctuation of the output with respect to the input and phase that contains the temporal relationship

between the two signals. Thus, normalized gain <0 dB indicates that RBF is stabilized with respect to blood pressure and hence that autoregulation is effective. The coherence function assesses the degree to which the data are related and provides information about the confidence one may have in the transfer function analysis. A high coherence at any frequency indicates that the input and output signals are closely and linearly related; reduced coherence can indicate the presence of noise, unrelated signals, or increased dynamic complexity.

Heretofore, all transfer function and correlation analyses of renal autoregulation have relied on the calculation of time-invariant linear transfer functions (TITF) and time-invariant linear coherence functions (TICF). These traditional methods assume that the system is linear, and that its dynamic characteristics do not vary with time (e.g., the system is stationary). Although both assumptions are questionable in the context of renal autoregulation, TITF and TICF analyses have proven to be useful tools in the study of renal hemodynamics (reviewed in Ref. 9). For example, a recent study using these time-invariant methods has reported conclusive evidence of differences in transfer function gains and coherence values between Sprague-Dawley rats (SDR) and spontaneously hypertensive rats (SHR), as well as rats with congestive heart failure, both with and without renal sympathetic denervation (13). This study also showed significantly increased coherence following renal denervation (13).

However, TICF typically reports low coherence at frequencies <0.05 Hz, in the region of the spectrum where TGF is operative, and often in the band from 0.1 to 0.2 Hz where the myogenic mechanism operates (e.g., see Ref. 16). Such a low coherence is generally held to severely limit the confidence one can place in the transfer function analysis. The low coherence has been attributed to the presence of significant nonlinearities in the autoregulatory mechanisms, because high coherence is routinely reported at higher frequencies. Previous studies examining nonlinear behavior of RBF dynamics used time-invariant analytical techniques so any time-varying behavior would have been interpreted as nonlinearities. Time-frequency mapping of the pressure and RBF (11, 33), as well as visual examination of many experimental records, suggests that time-varying behavior contributes substantially to dynamic complexity.

We have recently developed methods to compute time-varying transfer functions (TVTF) and time-varying coherence functions (TVCF) that are accurate and provide high frequency

Address for reprint requests and other correspondence: K. H. Chon, Dept. of Biomedical Engineering, SUNY at Stony Brook, HSC T18, Rm. 030, Stony Brook, NY 11794-8181 (e-mail: ki.chon@sunysb.edu).

The costs of publication of this article were defrayed in part by the payment of page charges. The article must therefore be hereby marked “advertisement” in accordance with 18 U.S.C. Section 1734 solely to indicate this fact.

and time resolution (31, 32). In this investigation, we used these methods to analyze whole kidney blood flow data collected from SDR and SHR. Our goal is to test the hypotheses that 1) there is biologically significant nonstationarity in RBF dynamics of normotensive and hypertensive rats, 2) this nonstationarity accounts for some of the insensitivity of TITF analysis to known modulators of autoregulation, and 3) the greater dynamic complexity of RBF dynamics in SHR results at least in part from increased nonstationarity.

## METHODS

**Experimental procedures.** Records of RBF and arterial pressure from seven SDR and six SHR were analyzed. In these records, an exogenous forcing of blood pressure was imposed to increase the power bandwidth to permit calculation of reliable transfer functions. The data were collected for a previously published study in which they were analyzed with time-invariant methods and where details of the experimental protocols are presented (3, 17). We have used the previously published data because one of our aims was to provide a direct comparison of the time-varying approaches to the TITF and TICF estimates since the latter calculations were based on the same data used in this work. These data have been used to assess how effectively a variety of techniques are to extract mechanistic insight from pressure-flow time series (5, 24, 27, 33). Here, the methods will be briefly summarized.

**Animal preparation.** The study was approved by the Animal Care Committees of the University of Southern California, and was conducted under the guidelines concerning the use of animals in research and teaching and the United States Public Health Service National Institutes of Health Guide for the Care and Use of Laboratory Animals. Experiments were performed on male SDR and SHR, 14–18 wk age and 250–300 g body wt. The rats had free access to food and water before the experiments. Anesthesia was induced by placing each rat in a chamber containing 5% halothane administered in 25% O<sub>2</sub>-75% N through a Fluotec Mark-3 vaporizer. A tracheostomy was performed, and a small animal respirator was adjusted to maintain arterial blood pH between 7.35 and 7.45 with a mixture of 25% O<sub>2</sub>-75% N. The final concentration of halothane needed to maintain sufficient anesthesia was ~1%. A polyethylene catheter was placed in the right jugular vein for infusions. After a priming dose of 6 mg gallamine triethiodide (Flaxedil) in 1 ml 0.9% saline, a continuous intravenous infusion of 60-mg gallamine triethiodide in 10 ml 0.9% saline was given at 20  $\mu$ l/min. Body temperature was maintained at 37°C by a servocontrolled heating table. The left kidney was exposed through a flank incision, immobilized with a lucite ring, and superfused with saline preheated at 37°C. Data acquisition started after a recovery period of 45 min.

**Forcing of the arterial blood pressure and whole kidney pressure and blood flow measurement.** Measurements of RBF and arterial pressure were made while broad-band fluctuations were induced in the distal aorta. A catheter was inserted into the superior mesenteric artery for measurement of the renal perfusion pressure since broad-band pressure fluctuations were induced in the distal aorta. The pressure in the superior mesenteric artery represents a kidney-filtered version of the broad-band pressure induced in the distal aorta. The left kidney was denervated and fitted with an electromagnetic flow probe. The aorta below the renal arteries was cannulated with a blood-filled catheter connected to a bellows pump, which in turn was driven by a computer-controlled motor. The blood was obtained from a donor rat on the day of the experiment. The input to the bellows pump was derived from a constant-switching-pace symmetric random input applied at 2 Hz and exhibited the spectral properties of band-limited white noise. Similar blood pressure power spectra were achieved in the SDR and SHR.

**Data analysis.** The arterial pressure and blood flow data were recorded on magnetic tape and digitized off-line. At that time, the signals were passed through a second-order low-pass Butterworth filter with cutoff at 1.5 Hz. The sampling rate for the blood pressure and flow measurements was ~9 Hz. Data were then preprocessed by low-pass filtering to 0.5 Hz and resampling to 1 Hz. Finally, each 1,024-point time series was subjected to low-order trend removal and normalized to zero mean and unit variance.

Statistical analysis was performed with a Student's *t*-test for unpaired data ( $n = 7$  for SDR and  $n = 6$  for SHR). To examine the time-varying nature of RBF dynamics, individual frequency vectors were extracted from the TVTF and TVCF and the means and standard deviations of these vectors were compared statistically.  $P < 0.05$  was considered statistically significant. All data are presented as means  $\pm$  SE.

**TVTF and TVCF.** Estimation of TVTF is based on a model-based approach known as the time-varying autoregressive moving average (TVARMA) model that has been reported in detail elsewhere (32). Similarly, details of the TVCF algorithm are reported elsewhere (31). However, we provide details of both TVTF and TVCF algorithms in APPENDIX A for the convenience of the readers. The TVTF and TVCF can be estimated via Eq. A6 and Eq. A7, respectively. The inverse Fourier transform of Eq. A6 represents the time-domain counterpart of the TVTF, and it is defined as the time-varying impulse response function. For example, a step response of the system can be obtained by integration of the impulse response function.

## RESULTS

**Application of TVTF.** Representative TVTFs of SDR and SHR are shown in Figs. 1 and 2, respectively, as both magnitude and contour plots. For both SDR and SHR, the characteristic resonance peak is seen at ~0.2 Hz (5, 17). In both strains, gain magnitude declines sharply with decreasing frequency, indicating efficient autoregulation of RBF. Very low frequency fluctuations of TVTF gain magnitude are evident in both strains, and these fluctuations give the appearance of being periodic with a period of ~200 to 300 s. In contrast, SHR exhibit much greater temporal variation in gain magnitude at frequencies above ~0.02 Hz. Figure 3 illustrates the time-varying impulse response functions for these two rats. A time-varying impulse response function is the time domain counterpart of the TVTF, and it is the predicted response to a large, brief pulse in blood pressure. In both rats, predicted blood flow shows a rapid rise and fall with a marked undershoot and damped oscillations, whose period is consistent with the myogenic mechanism, during the relaxation to baseline. Note that the predicted impulse response is more stable over time in the SDR compared with the SHR, another indication that autoregulation in SD rats is more stationary than in SHR.

**Quantification of nonstationarity.** To quantify nonstationarity between the two strains of rats, we tracked the peak amplitude within the myogenic (0.1–0.3 Hz) frequency ranges for each time point. For TGF, tracking of the peak amplitude was not done since there was no obvious resonance peak associated with it. The method is illustrated in Fig. 4, *left*, which shows peak amplitude variations as a function of time for all SDR (black line) and SHR (gray line). The peak amplitude variations are greater for SHR than SDR. Fig. 4, *middle* and *right*, show minimum amplitude variations in the frequency range associated with the myogenic and TGF, respectively, for both SDR (black line) and SHR (gray line). Physically, they represent efficiency of autoregulation attributable to the myogenic and TGF mechanisms, respectively. In

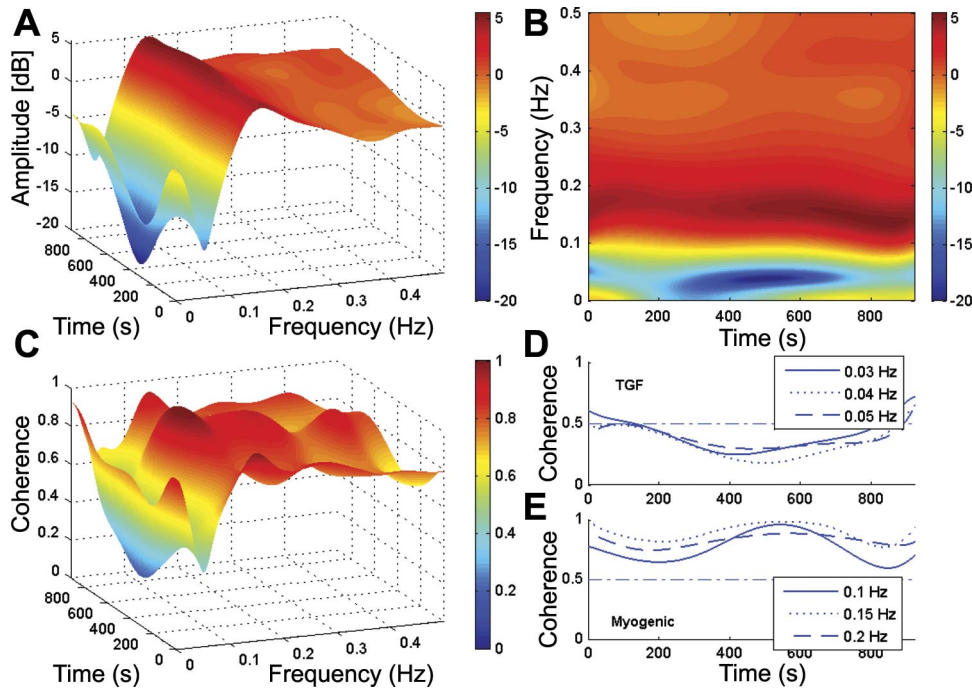


Fig. 1. Time-varying transfer functions (TVTF) of Sprague-Dawley rats (SDR; *A*: magnitude map, *B*: contour map), time-varying coherence function (TVCF; *C*), and time-varying coherence at 3 difference frequencies in tubuloglomerular (TGF) and myogenic frequency ranges (*D* and *E*), respectively.

both of these gain minimum plots, the average values were similar for SHR and SDR. However, variations are greater with SHR than SDR even though the power of the forced blood pressure fluctuations were comparable between SDR and SHR. Figure 5 shows quantitative analyses of plots shown in Fig. 4. There were significantly greater myogenic resonance amplitude peaks but with smaller variations for SDR than SHR. The greater significant variations in minimum gain values are also seen for SHR than SDR for the two frequency ranges associated with myogenic (Fig. 5, *middle*) and TGF (Fig. 5, *right*).

*Time-varying coherence function.* The TVCF is important because it provides insight into the correlation over time between the input and output signals (blood pressure and RBF, respectively). With TICF analysis, low coherence values can arise from noise, nonlinearity, and nonstationarity; hence, low coherence may not necessarily imply low correlation between the two signals. However, with the TVCF, one of the possible causes of the low coherence values, nonstationarity, can be eliminated. The estimated magnitude squared TVCFs for the two representative SDR and SHR are shown in Figs. 1*C* and

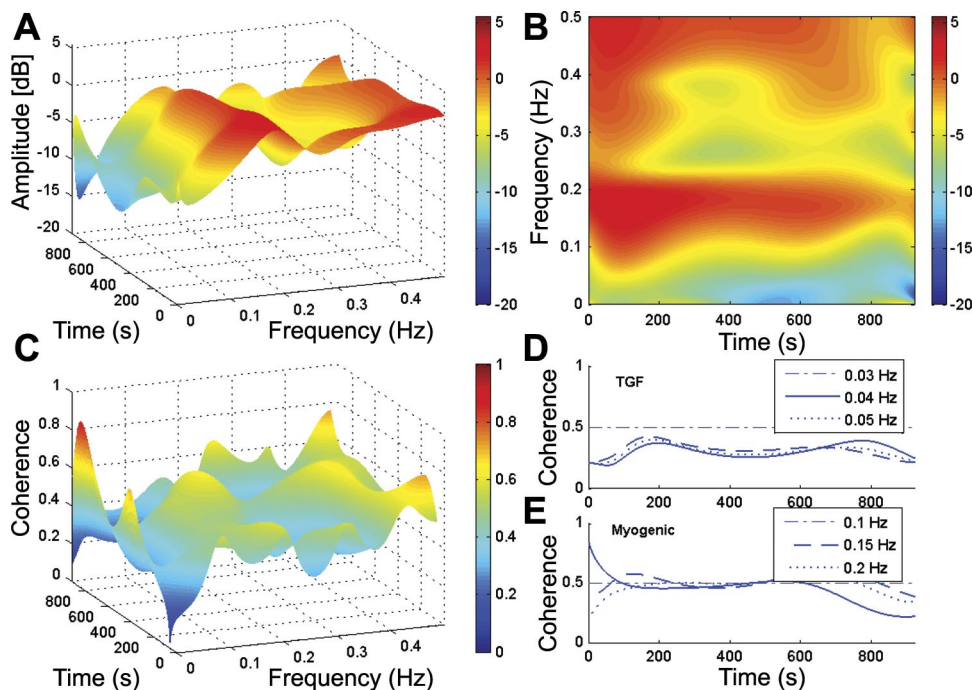
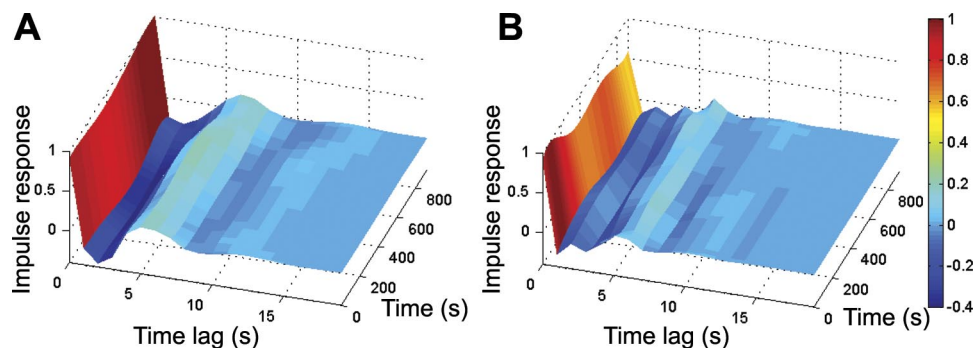


Fig. 2. TVTF of spontaneously hypertensive rats (SHR; *A*: magnitude map, *B*: contour map) and TVCF (*C*) and TVC at 3 difference frequencies in TGF and myogenic frequency ranges (*D* and *E*), respectively.

Fig. 3. Time-varying impulse response functions of SDR (A) and SHR (B).



2C, respectively. Note that these are the same animals subjected to TVTF analysis (Fig. 1 and 2), and recall that coherence  $>0.5$  is generally considered to be sufficient to permit the assumption of system linearity. For SDR, the TVCF of the MYO are consistently  $>0.5$  throughout the time and frequency duration except for frequencies below 0.05 Hz, a region where coherence is expected to be reduced by autoregulatory adjustments in RBF (thus giving a low signal-to-noise ratio). For SHR, the coherence values are highly variable, usually  $<0.5$ , and have even smaller values at frequencies  $<0.05$  Hz. Figs. 1D and 2D show frequency slices of the TVCF at 0.03, 0.04, and 0.05 Hz, the frequency range where the TGF mechanism is known to operate. Fig. 1E illustrates frequency slices of the TVCF with the myogenic frequency band at 0.1, 0.15, and 0.2 Hz. For the myogenic mechanism of SDR, high coherence values are observed for all times although they vary from a high value of 1 to a low value of 0.6. For the myogenic mechanism of SHR, TVCF values are lower than for SDR and fluctuate around 0.5. In both strains, coherence within the TGF frequency band is lower and more time-dependent than in the myogenic frequency band. TGF in the SDR starts at a high coherence value, but with time transitions to lower coherence values. The TGF band of SHR, while time varying, shows consistently low coherence values. It is important to note that in both strains the times at which coherence is low correspond to the times at which the TVTF analysis (Fig. 1) indicate the most effective regulation of RBF. Furthermore, the very slow periodic variation evident in TVTF gain magnitude is also apparent in the TVCF. Hence, although the overall lower coherence in this SHR suggests that its autoregulatory systems are more nonlinear than in the SDR, much of the temporal

variation in both strains appears to be related to the very low frequency fluctuations in autoregulatory gain.

As shown in Fig. 6A, coherence values for the myogenic mechanism are consistently  $>0.5$  for the normotensive rats and usually  $<0.5$  for SHR (5 of 6 rats). For TGF, four out of seven normotensive rats exhibited coherence values  $>0.5$  while five out of six SHR exhibited coherence values  $<0.5$ . Fig. 6B provides mean TVCF values (averaged across all times) in the frequency ranges associated with the myogenic and TGF mechanisms for rats in both groups. The mean TVCF values for the myogenic mechanism are significantly greater for normotensive than hypertensive rats, and while the same is true for TGF, this increase is statistically nonsignificant.

## DISCUSSION

The present study is the first systematic investigation of the time-varying properties of the renal autoregulatory mechanisms. Using recently-developed TVTF and TVCF approaches (31, 32), we were able to critically examine the stationarity of the TGF and myogenic autoregulatory mechanisms, to assess the extent that nonstationarities contributes to autoregulatory effectiveness and dynamic complexity. Based on information from studies of nonlinear dynamics (4, 6, 7, 21, 24, 28, 30) and from time-frequency mapping (11, 33), we predicted greater time-varying content in SHR than in SDR rats. The main findings of this study are that autoregulatory dynamics in both strains show significant variation over time, in the form of intermittent peaks and slow oscillations in transfer function gain. Furthermore, SHR exhibit significantly more temporal variability than SDR. Finally, compared with SDR, the major-

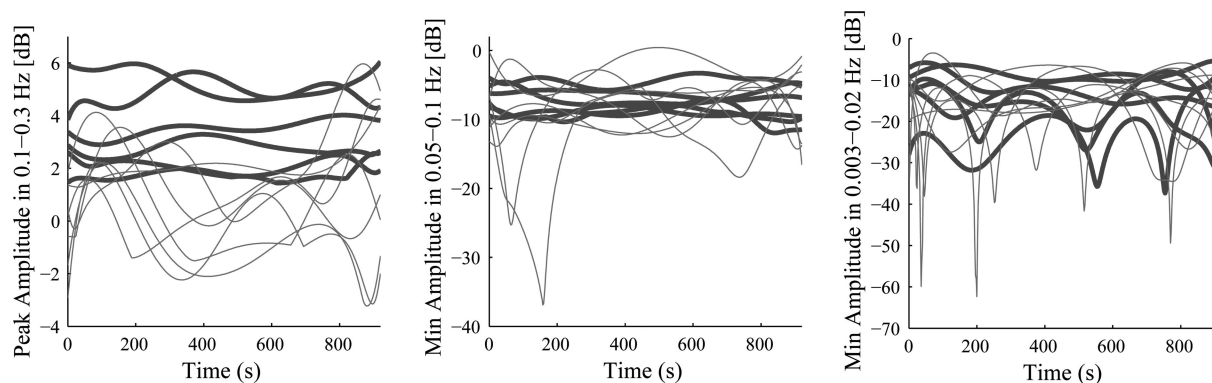


Fig. 4. Comparison of peak amplitudes of TVTF between SDR and SHR at the frequency range associated with the myogenic mechanism (left). Middle and right: variations of minimum TVTF amplitudes in the frequency ranges associated with the myogenic and TGF mechanisms, respectively.

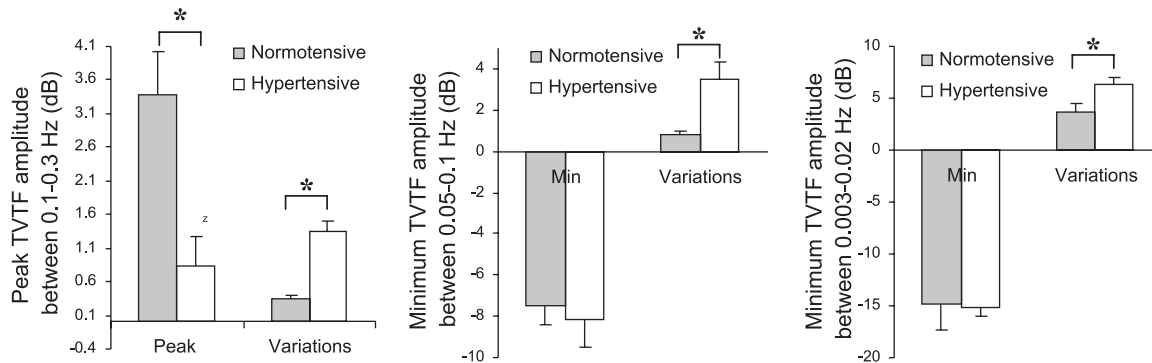


Fig. 5. Statistical comparison of peak amplitudes of TVTF between SDR and SHR at the frequency range associated with the myogenic mechanism (*left*). *Middle* and *right*: statistical comparison of minimum TVTF amplitudes between SDR and SHR in the frequency ranges associated with the myogenic and TGF mechanisms, respectively. \* $P < 0.05$ .

ity of SHR exhibit low time-varying coherence values in the frequency range associated with the myogenic and TGF mechanisms, including intervals in which gain is relatively stable, which suggests that the autoregulatory mechanisms in SHR are intrinsically more nonlinear than in normotensive SDR rats. The results of this study support and expand upon recent investigations of nonlinearity and nonstationarity in renal hemodynamics. Zou et al. (33) used various time-varying spectral techniques to demonstrate that both SDR and SHR exhibit time-varying renal autoregulatory responses, with greater nonstationarity observed in SHR. Cupples et al. (11) employed a different technique, Wigner-Ville spectra, to illustrate the time-varying properties of the renal autoregulatory mechanism in SDR.

The TVTF quantifies the gain relationship between RBF and arterial blood pressure at each instant in time and thus detects intermittent gain changes that occur. The TVTF approach used in this paper overcomes a fundamental limitation of short-time Fourier transform, a method widely used in time-varying spectral analysis. Using the short-time Fourier transform, a TVTF can be computed by division of time-varying cross spectrum (between blood flow and pressure) by the time-varying spectrum of a blood pressure signal. However, this approach leads to unreliable TVTF estimates in many cases, as the resolution in time and frequency vary inversely and is data length dependent. The result is that one cannot obtain simultaneous high time and frequency resolution (8). In contrast, our method provides excellent time and frequency resolution, provided that proper model coefficients [ $a(k, n)$  and  $b(k, n)$ ] in Eq. A1 have been determined. Determination of the proper

model coefficients of the TVTF utilized in this study has been previously demonstrated (32).

The observation that both the TGF and myogenic autoregulatory systems exhibit substantial time variability is not surprising given that these two mechanisms interact via a nonlinear feedback process to minimize blood flow variations despite forced blood pressure fluctuations (7, 14, 21, 24, 27). A prominent feature of the TVTF is the very low frequency modulation of gain magnitude in the TGF frequency range in both SDR and SHR, and in the myogenic frequency range in SHR. The origin of this phenomenon is unclear, but very low frequency oscillations in RBF have been noted in conscious dogs and attributed to fluctuations in ambient levels of vasoactive agents (28). Very low frequency oscillations in RBF have also been induced by blood pressure forcing (11), and may be related to the slow component of renal autoregulation suggested by Just and coworkers (18, 19). Furthermore, because of the known interactions between the TGF and myogenic mechanisms, the fact that both autoregulatory systems exhibited some degree of nonstationarity is to be expected. In the steady-state, both experimental and modeling studies have shown a strong dependence of the myogenic autoregulatory system on TGF, such that myogenic compensation is enhanced when the TGF system is stimulated (15, 23, 25). Similarly, both the myogenic mechanism (25) and TGF (31) are extensively modulated by ANG II, the generation of which is at least partly TGF dependent. Furthermore, there are nonlinear interactions between these two systems that produce spectral peaks (7, 21, 24) and changes in overall system behavior (19, 20). In addition, the state of the TGF system appears to modulate the

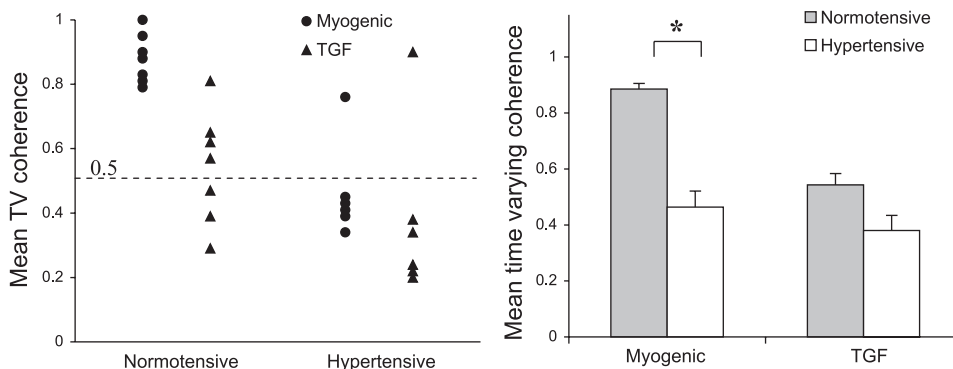


Fig. 6. Distribution of mean time-varying coherence values in the myogenic and TGF frequency ranges for SDR and SHR, respectively (A); Mean time-varying coherence values in the frequency ranges associated with the myogenic and TGF mechanisms for rats in both groups (B). \* $P < 0.05$ .

resonant frequency of the myogenic mechanism (26, 27). Hence, even if the strength of either of these two mechanisms is modulated over time by exogenous factors, it is to be expected that the state and responsiveness of the other mechanism will be affected.

It is important to recognize that information concerning this kind of time-varying behavior would be lost in a time-invariant transfer function, which would represent just the time average of features evident in a TVTF. As a result, the time-resolution of time-invariant methods is very limited, and any nonstationarity that is present may distort the spectra and introduce artifactual spectral complexity (21). Nevertheless, time-invariant methods have played an important role in elucidating the dynamics of renal autoregulation. Several laboratories (10, 12, 16) first used the TITF to demonstrate operative dynamics of renal autoregulation. The simple calculation of TITF based on the ratio of the spectra of the blood pressure and flow, and insights it provided, led other investigators to look for differences in transfer function gain between SDR and SHR (5), before and after administration of pharmacological agents (11), between healthy rats and rats with renal disease (2, 20), and before and after renal denervation in several species (13). In the aforementioned studies, statistically significant differences were not always found using TITF, although in each case there was good reason to expect such differences, which suggests that the TITF method may be not be sensitive enough to detect significant changes in dynamics when the data are even modestly nonstationary. Thus, TVTF methods are preferable, and it would seem prudent to employ time-varying spectral methods to verify that negative conclusions are not a consequence of nonstationarity.

Analysis of coherence with time-invariant methods has been used to assess linearity of the autoregulatory mechanisms (5, 10, 13). Two of these studies have reported higher coherence values in the frequency ranges associated with the myogenic and TGF mechanisms for SDR than for SHR (10, 13). Furthermore, it has been shown that for both SDR and SHR, coherence values are generally  $>0.5$  at frequencies faster than 0.1 Hz and are consistently lower at frequencies slower than 0.05 Hz. The low coherence values observed with the TGF mechanism for both SDR and SHR have been attributed to the nonlinear dynamics of TGF (6, 7), and, in some cases, coherence values were lower for SHR than for SDR (4, 13). A report by Yip and Holstein-Rathlou (30) has suggested that the lower coherence values in SHR may, in part, be due to chaotic behavior of TGF in this strain. Our results using the TVCF are generally consistent with these findings. In several frequency bands, we found coherence to exhibit more time-varying behavior and to be significantly lower in SHR than in SDR. Because the TVCF does not assume stationarity, the fact that we still observe low coherence values in SHR is consistent with the idea that the autoregulatory systems in SHR are more nonlinear than in normotensive rats.

Nevertheless, there are two notable differences between our study and previous investigations using TITF. First, high coherence values of the myogenic mechanism were consistently observed in both SHR and SDR in previous studies using TITF, whereas this was only true for SDR with TVCF analysis. Second, unlike previous studies, we observe high coherence values for the TGF mechanism in most SDR (4 out of 7). These observations suggest that autoregulatory mechanisms may ex-

hibit quasilinear control properties in SDR and nonlinear control properties in SHR. While further analyses are required on diverse sets of experimental data, the present results suggest that autoregulatory mechanisms in hypertension are dominated by nonlinear control processes. It is unclear as to what or why autoregulatory mechanisms exhibit nonlinear control properties in SHR, although two recent hypotheses may be relevant. In a simulation study, Ditlevsen et al. (14) proposed that the nonlinear dynamics exhibited by SHR can be explained by relatively large and rapid random fluctuations in TGF system gain, a parameter chosen "to represent mechanisms not explicitly included in the model" (14). Layton et al. (21) have suggested that a sufficient explanation for the irregular fluctuations in the TGF system in SHR may involve resetting and temporal variation in TGF gain and/or time delays in coupled nephrons that may result in abrupt switching between multiple stable oscillatory modes. It is interesting that both of these hypotheses involve parameter nonstationarity. Hence, the availability of high resolution time-varying methods for spectral and transfer function analysis will be of value in experimental investigations of these hypotheses.

In summary, nonstationarities in both the myogenic and TGR feedback mechanisms were observed in normotensive rats, while the nonstationary characteristics in hypertensive rats were significantly greater, as both mechanisms displayed very low frequency oscillations in gain and coherence. Furthermore, hypertensive rats appear to have lower time-varying admittance gain (and thus less variation in blood flow), especially in the myogenic frequency range and consistently lower TVCF values than normotensive rats. Our results indicate that although the autoregulatory dynamics of normotensive rats are often quasilinear, hypertensive rat dynamics are much more complicated and require analysis with methods designed to capture both nonlinear and time-varying system dynamics.

### *Perspectives and Significance*

It has been apparent for some time that RBF autoregulation exhibits dynamics that are more complex than can be captured by linear, time-invariant analysis. To some extent this complexity arises out of the system's anatomy; both TGF and the myogenic mechanism operate on afferent arteriolar resistance, while the TGF sensor is downstream of all other components of the combined system. But it is also clear that the complexity of RBF dynamics is greater in hypertensive than in normotensive rats (3, 4). To a very large extent, previous studies addressing this complexity have lumped together nonlinear and nonstationary (time-varying) behavior and have not differentiated between the two. The present results show that autoregulatory efficiency shows substantial variation in time in both normotensive (SDR) and hypertensive (SHR) rats. In SDR the nonstationarity accounts for a large fraction of the previously observed dynamic complexity was not captured by TITF. In SHR, however, although the time-variance of autoregulation is even greater than that in SDR, there remains a substantial fraction of dynamic complexity that is not explained by time-variance. Clearly, future studies will need to address both mechanisms and implications of time-variance in autoregulatory efficiency.

## APPENDIX A

Estimation of TVTF is based on a model-based approach known as the TVARMA model (32). While theoretically it is possible to calculate TVTF using the division of the time-varying cross spectrum by the time-varying auto spectrum, it is impractical because most time-varying spectra exhibit zero power, which precludes calculation of a TVTF.

The TVARMA process is represented by the following equation

$$y(n) = \sum_{i=1}^P a(i, n)y(n-i) + \sum_{j=0}^Q b(j, n)x(n-j) + e(n) \quad (A1)$$

where  $a(i, n)$  and  $b(j, n)$  are the TVARMA coefficients to be determined, respectively, and are functions of time. Indexes  $P$  and  $Q$  are the maximum model orders of the autoregressive and moving average models, respectively. Variables  $y(n)$  (blood flow) and  $x(n)$  (blood pressure) represent output and input signals, respectively. The term  $e(n)$  is the prediction error. The time-varying coefficients  $a(i, n)$  and  $b(j, n)$  are expanded onto a set of basis functions  $\pi_k(n)$

$$\begin{aligned} a(i, n) &= \sum_{k=0}^V \alpha(i, k)\pi_k(n) \\ b(j, n) &= \sum_{k=0}^V \beta(j, k)\pi_k(n) \end{aligned} \quad (A2)$$

where  $\alpha(i, k)$  and  $\beta(j, k)$  represent the expansion parameters with  $V$  as the maximum number of basis sequences. Substituting Eq. A2 into Eq. A1, we obtain the following

$$\begin{aligned} y(n) &= \sum_{i=1}^P \sum_{k=0}^V \alpha(i, k)\pi_k(n)x(n-i) \\ &+ \sum_{j=0}^Q \sum_{k=0}^V \beta(j, k)\pi_k(n)x(n-j) + e(n) \end{aligned} \quad (A3)$$

For data analyses, we have used Legendre polynomials as they are most appropriate for smoothly changing dynamics. APPENDIX B details the use of Legendre functions and provides information on how to choose the proper number of  $V$  in Eq. A3.

Once proper basis functions,  $\pi_k(n)$ , have been chosen (Legendre), we create new variables

$$\begin{aligned} y_k(n-i) &= \pi_k(n)y(n-i) \\ x_k(n-j) &= \pi_k(n)x(n-j) \end{aligned} \quad (A4)$$

Substituting Eq. A4 into Eq. A3 results in the following expression

$$y(n) = \sum_{i=1}^P \sum_{k=0}^V \alpha(i, k)y_k(n-i) + \sum_{j=0}^Q \sum_{k=0}^V \beta(j, k)x_k(n-j) + e(n) \quad (A5)$$

Equation A5 shows that the TVARMA model can now be considered to be a TIV-ARMA model since  $\alpha(i, k)$  and  $\beta(j, k)$  are not functions of time. Thus, the task simplifies to solving for parameters  $\alpha(i, k)$  and  $\beta(j, k)$ , which can be more effectively estimated using the optimal parameter search algorithm (22). For details of the optimal parameter search algorithm concerning model order determination and the selection of only the significant model terms, the reader is referred to Lu et al. (22).

Once the time-varying ARMA coefficients are identified, the TVTF can be easily estimated using the following

$$H(n, e^{j\omega}) = \frac{\sum_{k_2=0}^Q b(k_2, n)e^{-j\omega k_2}}{\sum_{k_1=1}^P a(k_1, n)e^{-j\omega k_1}} \quad (A6)$$

The norm of  $H(n, e^{j\omega})$ ,  $\|H(n, e^{j\omega})\|$  represents the time-varying gain of the linear time-varying system, and the angle of  $H(n, e^{j\omega})$ ,  $\angle H(n, e^{j\omega})$  represents the time-varying phase of the linear time-varying system.  $H(n, e^{j\omega})$  is an extension of the linear time-invariant system such that the single variable, either time or frequency, is mapped to the two variables of time and frequency.

TVCF. In this section, we demonstrate that the TVCF can be obtained by using the TVTF relationships (43). To demonstrate the use of the TVTF in obtaining the TVCF, we first define the TVCF via the nonparametric time-frequency spectra

$$|\gamma(t, f)|^4 = \left( \frac{|S_{xy}(t, f)|^2}{S_{xx}(t, f)S_{yy}(t, f)} \right) \left( \frac{|S_{yx}(t, f)|^2}{S_{yy}(t, f)S_{xx}(t, f)} \right) \quad (A7)$$

where  $S_{xy}(t, f)$  and  $S_{yx}(t, f)$  represent the time-frequency cross spectrum, and  $S_{xx}(t, f)$  and  $S_{yy}(t, f)$  denote the auto spectrum of the two signals  $x$  and  $y$ , respectively. The above expression  $\frac{|S_{xy}(t, f)|^2}{S_{xx}(t, f)S_{yy}(t, f)}$  is the coherence function when  $x$  is considered as the input and  $y$  as the output, while  $\frac{|S_{yx}(t, f)|^2}{S_{yy}(t, f)S_{xx}(t, f)}$  is the coherence function when  $y$  is considered as the input and  $x$  as the output. We note that for a linear time-varying system with  $x$  and  $y$  as the input and output signals, respectively, the following TVTF in terms of time-frequency spectra can be obtained

$$H_{xy}(t, f) = \frac{S_{xy}(t, f)}{S_{xx}(t, f)} \quad (A8)$$

where  $H_{xy}(t, f)$  denotes the TVTF from the input  $x$  to the output  $y$  signals. Similarly, if we reversed the input and output relationship such that the variables  $y$  and  $x$  represent input and output signals, respectively, then the following TVTF can be obtained

$$H_{yx}(t, f) = \frac{S_{yx}(t, f)}{S_{yy}(t, f)} \quad (A9)$$

The desired relationship of Eq. A7 can be obtained by multiplying the two TVTF relationships of Eq. A8 and Eq. A9, which yields

$$\begin{aligned} |H_{xy}(t, f)H_{yx}(t, f)|^2 &= \left| \frac{S_{xy}(t, f)}{S_{xx}(t, f)S_{yy}(t, f)} \right|^2 \cdot \left| \frac{S_{yx}(t, f)}{S_{yy}(t, f)S_{xx}(t, f)} \right|^2 \\ &= \frac{|S_{xy}(t, f)|^2}{S_{xx}(t, f)S_{yy}(t, f)} \cdot \frac{|S_{yx}(t, f)|^2}{S_{yy}(t, f)S_{xx}(t, f)} = |\gamma(t, f)|^4 \end{aligned} \quad (A10)$$

Thus, time-varying magnitude squared coherence,  $|y(t, f)|^2$ , is then obtained by multiplying the two transfer functions,  $|H_{xy}(t, f)H_{yx}(t, f)|$ , together.

Given the relationship of Eq. A10, a high resolution TVCF via the parametric TVTF can be obtained. Specifically, each of the two transfer functions in Eq. A10 can be obtained using autoregressive moving average models such that

$$y(n) = \sum_{i=1}^P a(n, i)y(n-i) + \sum_{j=0}^Q b(n, j)x(n-j) + e_1(t) \quad (A11)$$

$$x(n) = \sum_{i=1}^P \alpha(n, i)x(n-i) + \sum_{j=0}^Q \beta(n, j)y(n-j) + e_2(t)$$

where ARMA models of the top and bottom expressions in Eq. A11 represent  $y(n)$  as the output and  $x(n)$  as the output, respectively. Given the ARMA models of Eq. A11, the two transfer functions of Eq. A10 can be obtained by the following equation

$$H_{xy}(n, e^{j\omega}) = \frac{B(e^{j\omega})}{A(e^{j\omega})} = \frac{\sum_{i=0}^Q b(n, i)e^{-j\omega i}}{\sum_{i=0}^P a(n, i)e^{-j\omega i}} \quad (A12)$$

$$H_{yx}(n, e^{j\omega}) = \frac{\beta(e^{j\omega})}{\alpha(e^{j\omega})} = \frac{\sum_{i=0}^Q \beta(n, i)e^{-j\omega i}}{\sum_{i=0}^P \alpha(n, i)e^{-j\omega i}}$$

## APPENDIX B

*Legendre polynomials.* Recurrence relations to generate Legendre polynomials are provided below

$$P_0(x) = 1$$

$$P_1(x) = x$$

$$(l + 1)P_{l+1}(x) = (2l + 1)xP_l(x) - lP_{l-1}(x)$$

We chose Legendre basis functions for their exponential characteristics, which make them especially suitable for modeling biological systems (31, 32). The number of coefficients estimated depends on the choice of TVARMA model orders  $P$  and  $Q$  as well as the selection of  $V$  in Eq. A3. Specifically, the total number of coefficients to be estimated is  $P(V+1) + (Q+1)(V+1)$ . Note that other time-varying approaches utilize far more parameters than does our approach (31, 32). The determination of the number of time-varying basis functions  $V$  requires some a priori knowledge of the nonstationarities in a system. We based our choice of the appropriate values of  $V$  on the mean square error (MSE) criterion. We have shown that the MSE values gradually decrease as the number of basis sequences increase, but when  $V$  is too large, the MSE value will become exorbitantly large. Thus, the approach to take to determine the sufficient number of  $V$  is to increase  $V$  until the MSE value no longer decreases.

## GRANT

This research is supported by National Heart, Lung, and Blood Institute Grant HL-69629.

## REFERENCES

1. Abu-Amarah I, Ajikobi DO, Bachelard H, Cupples WA, Salevsky FC. Responses of mesenteric and renal blood flow dynamics to acute denervation in anesthetized rats. *Am J Physiol Regul Integr Comp Physiol* 275: R1543–R1552, 1998.
2. Bidani AK, Hacioglu R, Abu-Amarah I, Williamson GA, Loutzenhiser R, Griffin KA. “Step” vs. “dynamic” autoregulation: implications for susceptibility to hypertensive injury. *Am J Physiol Renal Physiol* 285: F113–F120, 2003.
3. Chen YM, Holstein-Rathlou NH. Differences in dynamic autoregulation of renal blood flow between SHR and WKY rats. *Am J Physiol Renal Fluid Electrolyte Physiol* 264: F166–F174, 1993.
4. Chon KH, Chen YM, Holstein-Rathlou NH, Marmarelis VZ. Nonlinear system analysis of renal autoregulation in normotensive and hypertensive rats. *IEEE Trans Biomed Eng* 45: 342–353, 1998.
5. Chon KH, Chen YM, Holstein-Rathlou NH, Marsh DJ, Marmarelis VZ. On the efficacy of linear system analysis of renal autoregulation in rats. *IEEE Trans Biomed Eng* 40: 8–20, 1993.
6. Chon KH, Chen YM, Marmarelis VZ, Marsh DJ, Holstein-Rathlou NH. Detection of interactions between myogenic and TGF mechanisms using nonlinear analysis. *Am J Physiol Renal Fluid Electrolyte Physiol* 267: F160–F173, 1994.
7. Chon KH, Raghavan R, Chen YM, Marsh DJ, Yip KP. Interactions of TGF-dependent and myogenic oscillations in tubular pressure. *Am J Physiol Renal Physiol* 288: F298–F307, 2005.
8. Cohen L. *Time-Frequency Analysis*. Upper Saddle River, NJ: Prentice-Hall, 1995.
9. Cupples WA, Braam B. Assessment of renal autoregulation. *Am J Physiol Renal Physiol* 292: F1105–F1123, 2007.
10. Cupples WA, Loutzenhiser RD. Dynamic autoregulation in the in vitro perfused hydronephrotic rat kidney. *Am J Physiol Renal Physiol* 275: F126–F130, 1998.
11. Cupples WA, Novak P, Novak V, Salevsky FC. Spontaneous blood pressure fluctuations and renal blood flow dynamics. *Am J Physiol Renal Fluid Electrolyte Physiol* 270: F82–F89, 1996.
12. Daniels FH, Arendshorst WJ, Roberds RG. Tubuloglomerular feedback and autoregulation in spontaneously hypertensive rats. *Am J Physiol Renal Fluid Electrolyte Physiol* 258: F1479–F1489, 1990.
13. DiBona GF, Sawin LL. Effect of renal denervation on dynamic autoregulation of renal blood flow. *Am J Physiol Renal Physiol* 286: F1209–F1218, 2004.
14. Ditlevsen S, Yip KP, Marsh DJ, Holstein-Rathlou NH. Parameter estimation of feedback gain in a stochastic model of renal hemodynamics: differences between spontaneously hypertensive and Sprague-Dawley rats. *Am J Physiol Renal Physiol* 292: F607–F616, 2007.
15. Feldberg R, Colding-Jorgensen M, Holstein-Rathlou NH. Analysis of interaction between TGF and the myogenic response in renal blood flow autoregulation. *Am J Physiol Renal Fluid Electrolyte Physiol* 269: F581–F593, 1995.
16. Holstein-Rathlou NH, Wagner AJ, Marsh DJ. Dynamics of renal blood flow autoregulation in rats. *Kidney Int Suppl* 32: S98–S101, 1991.
17. Holstein-Rathlou NH, Wagner AJ, Marsh DJ. Tubuloglomerular feedback dynamics and renal blood flow autoregulation in rats. *Am J Physiol Renal Fluid Electrolyte Physiol* 260: F53–F68, 1991.
18. Just A, Arendshorst WJ. Dynamics and contribution of mechanisms mediating renal blood flow autoregulation. *Am J Physiol Regul Integr Comp Physiol* 285: R619–R631, 2003.
19. Just A, Ehmke H, Toktomambetova L, Kirchheim HR. Dynamic characteristics and underlying mechanisms of renal blood flow autoregulation in the conscious dog. *Am J Physiol Renal Physiol* 280: F1062–F1071, 2001.
20. Karlsen FM, Leyssac PP, Holstein-Rathlou NH. Tubuloglomerular feedback in Dahl rats. *Am J Physiol Regul Integr Comp Physiol* 274: R1561–R1569, 1998.
21. Layton AT, Moore LC, Layton HE. Multistability in tubuloglomerular feedback and spectral complexity in spontaneously hypertensive rats. *Am J Physiol Renal Physiol* 291: F79–F97, 2006.
22. Lu S, Ju KH, Chon KH. A new algorithm for linear and nonlinear ARMA model parameter estimation using affine geometry. *IEEE Trans Biomed Eng* 48: 1116–1124, 2001.
23. Moore LC, Rich A, Casellas D. Ascending myogenic autoregulation: interactions between tubuloglomerular feedback and myogenic mechanisms. *Bull Math Biol* 56: 391–410, 1994.
24. Raghavan R, Chen X, Yip KP, Marsh DJ, Chon KH. Interactions between TGF-dependent and myogenic oscillations in tubular pressure and whole kidney blood flow in both SDR and SHR. *Am J Physiol Renal Physiol* 290: F720–F732, 2006.
25. Schnermann J, Briggs JP. Interaction between loop of Henle flow and arterial pressure as determinants of glomerular pressure. *Am J Physiol Renal Fluid Electrolyte Physiol* 256: F421–F429, 1989.
26. Sosnovtseva OV, Pavlov AN, Mosekilde E, Holstein-Rathlou NH, Marsh DJ. Double-wavelet approach to study frequency and amplitude modulation in renal autoregulation. *Physiol Res* 70: 031915, 2004.
27. Sosnovtseva OV, Pavlov AN, Mosekilde E, Holstein-Rathlou NH, Marsh DJ. Double-wavelet approach to studying the modulation properties of non-stationary multimode dynamics. *Physiol Meas* 26: 351–362, 2005.
28. Wagner CD, Persson PB. Nonlinear chaotic dynamics of arterial blood pressure and renal blood flow. *Am J Physiol Heart Circ Physiol* 268: H621–H627, 1995.
29. Wang X, Cupples WA. Interaction between nitric oxide and renal myogenic autoregulation in normotensive and hypertensive rats. *Can J Physiol Pharmacol* 79: 238–245, 2001.
30. Yip KP, Holstein-Rathlou NH. Chaos and non-linear phenomena in renal vascular control. *Cardiovasc Res* 31: 359–370, 1996.
31. Zhao H, Lu S, Zou R, Ju K, Chon KH. Estimation of time-varying coherence function using time-varying transfer functions. *Ann Biomed Eng* 33: 1582–1594, 2005.
32. Zou R, Chon KH. Robust algorithm for estimation of time-varying transfer functions. *IEEE Trans Biomed Eng* 51: 219–228, 2004.
33. Zou R, Cupples WA, Yip KP, Holstein-Rathlou NH, Chon KH. Time-varying properties of renal autoregulatory mechanisms. *IEEE Trans Biomed Eng* 49: 1112–1120, 2002.